

The chatter identification in end milling based on combining EMD and WPD

Changfu Liu¹ · Lida Zhu¹ · Chenbing Ni¹

Received: 1 November 2016 / Accepted: 4 January 2017 / Published online: 22 January 2017
© Springer-Verlag London 2017

Abstract On-line detection of chatter in the cutting process can identify the chatter in time or before the chatter happens, so the initiative to change the cutting parameters can be taken to avoid chatter and improve the surface quality. At present, time-frequency analysis technology is performed to extract the time-frequency features of chatter by scholars. With respect to the modal aliasing problem in the process of empirical mode decomposition (EMD), the chatter identification method of combining EMD and wavelet packets decomposition (WPD) is proposed to eliminate the influence of modal aliasing. To fully extract the main features of signal, the intrinsic mode functions (IMFs) changing consistent with power spectrum or amplitude-frequency are selected for signal reconstruction. Then, WPD is used in the reconstructed signal. The two times reconstruction of signal is based on wavelet packet node with the maximum energy. The distribution of frequency and energy in the time domain is presented by Hilbert Huang Transform (HHT) spectrum, and the mean value and standard deviation of the HHT spectrum are extracted as the feature vectors. The chatter features can be extracted from the original simulation signal by this method. Three groups of experiments with different cutting depth which are on behalf of the three cutting conditions (stable cutting, slight chatter, and severe chatter) were carried out. More cutting tests were carried out under the same cutting condition. Experimental results show that this method can be used to effectively identify the chatter features in milling process.

Keywords Chatter identification · Time-frequency analysis · EMD · WPD · HHT

1 Introduction

Chatter is a frequent phenomenon in machining processing, which will cause the decrease of surface quality. The prediction methods of chatter to solve the equations are a line of research, as is shown in [1–5]. A new dynamic model of tool and workpiece system to consider the thin-walled workpiece with curved surface is proposed by Yang [6]. A systematic study to comprehensively model the plowing and shearing mechanisms in milling process is performed in [7], where the plowing mechanism is modeled in a generalized way for predicting both the static plowing forces and the dynamic stability with the effect of the process damping. The stability lobe prediction methods are proposed by Wan [8] for the milling process with multiple delays, which are often induced by cutter run-out. The mechanics and dynamics of thread milling process are presented by Wang [9]. The process of wear during tap forming for threading of cold forged steel parts is presented by Bustillo [10] from an experimental and a data-mining perspective. The performance of different configurations and types of artificial neural networks (ANNs) for the prediction of dimensional error on inclined surfaces manufactured by ball-end milling is compared by Álvar [11]. A new integrated genetic programming and genetic algorithm approach to predict surface roughness in end-milling is proposed by Miran [12]. Some optimization algorithms are induced by [13, 14] for solving manufacturing optimization problems.

It is important to find the chatter in the machining process or before and some active measures such as changing the cutting parameters can be taken to avoid the chatter. A lot of

✉ Changfu Liu
liu1changfu@163.com

¹ School of Mechanical Engineering and Automation, Northeastern University, No. 3-11, Shenyang 110819, China

research on cutting chatter identification has been done by scholars. The signal processing method is used to extract the chatter features, regardless of which signal is chosen to identify chatter in the cutting process. The observer-based cutting force monitoring technology for full-closed controlled ball-screw-driven stages is proposed by Yamada [15]. An approach using a nonlinear delayed model that describes the tool oscillations due to self-excited vibrations in turning is proposed by Khasawneh [16]. An identification method using analytically calculated and experimentally obtained end point FRFs of the holder-tool assembly at free-free end conditions for contact parameters at holder-tool interface is presented by Matthias [17]. In mechanical processing, the chatter phenomenon is accompanied by the redistribution of frequency and energy as demonstrated [18]. For the signal feature selection and extraction, time-frequency technology is shown in [19–22]. The method of feature extraction based on support vector machine was proposed by Yao [23] and Peng [24]. The effect of tool edge radius on tool edge wear as well as the corresponding effects of tool edge wear on the cutting forces and the cutting vibrations have been investigated in [25], where both the traditional fast Fourier transform (FFT) technique and the modern discrete wavelet transform technique are used. The cutting force variation is described by Huang [26] based on time domain analysis, frequency domain analysis, and wavelet analysis to ascertain the effect of the cutting speeds on cutting stability. A generic chatter identification approach is proposed in [27], where the energy ratio of the dominant frequencies on the FFT spectrum is performed as occurrence of chatter. A simple method for the detection of milling chatter is presented by Zhang [28]. The assessment of milling process stability by recursive drawing method combined with Hilbert Huang transform was proposed by Rafal [29]. WPT worked as a preprocessor to denoise the measured signals was proposed by Cao [30] and the performance of the HHT was enhanced. Later, the ensemble empirical mode decomposition (EEMD) combined with the nonlinear energy entropy index was proposed to identify the chatter features as demonstrated [31]. Cao's method had problems such as selection problem of wavelet packet bases was put forwarded by Fu [32], so the method based on HHT and energy aggregation to characterize the energy distribution in milling process is proposed by them, Gaussian mathematical model is introduced to realize the automatic chatter identification. A chatter detection method is proposed by [33] based on synchrosqueezing transform (SST) of sound signals.

In summary, the redistribution of frequency and energy in the cutting process was shown by the time-frequency analysis technology, and it has been widely applied in chatter feature extraction in cutting process. The key of chatter identification is feature extraction, the state-of-art of feature extraction is to obtain chatter band. EMD is an effective method to obtain chatter band, but it is prone to the phenomenon of modal

aliasing as demonstrated in [34]. Modal aliasing refers to that an IMF characteristic contains different time scales, or similar time scale distributes in different IMFs. The two IMFs waveform result in adjacent aliasing and influence each other, so it is difficult to identify. Although EEMD which was used by Cao [31] is an improved method of EMD, the chatter band is not subdivided enough. So, the chatter identification method of combining EMD and WPD to eliminate the influence of modal aliasing and subdivide the frequency band is proposed in this paper.

The rest paper is organized as follows. The theoretical basis of EMD is firstly introduced, which shows that why EMD has problems of modal aliasing and WPD can solve it. To eliminate modal aliasing of EMD and subdivide the frequency, the chatter identification method of combining EMD and WPD is proposed. Then to illustrate the effectiveness of the method, simulation signals containing chatter information is verified and the process is introduced in detail. Next, milling experiments is carried out to further verify, HHT spectrum is acquired. Finally, the conclusive remarks are laid out.

2 Theoretical basis of EMD and WPD

2.1 EMD

The complex signal $z(t)$ corresponding to a real signal $x(t)$ is defined according to [32]:

$$z(t) = x(t) + jy(t) = \sqrt{x^2(t) + y^2(t)}e^{j\theta(t)} \quad (1)$$

And the instantaneous frequency is defined as the derivative of the instantaneous phase, that is,

$$\tilde{\omega}(t) = \frac{d\left(\arctan \frac{y(t)}{x(t)}\right)}{dt} \quad (2)$$

The purpose of EMD is to obtain the instantaneous frequency. $x(t)$ can be expressed as a sum of components of IMF, and a residual term,

$$x(t) = \sum_{j=1}^n C_j(t) + r_n(t), \quad (3)$$

where $r_n(t)$ is the residual, which represents the average trend; each segment contains different frequency components which are given by each IMF component $C_j(t)$. The distribution of the different frequency components is changed with the signal itself.

2.2 WPD

Because only low-frequency parts of signal are further decomposed by the orthogonal wavelet transform, the high frequency parts of signal are no longer continue to be decomposed, so the low frequency signal can be well characterized by wavelet transform, but signal containing a lot of detail information cannot be well decomposed by wavelet transform, such as non-smooth mechanical vibration signal, remote sensing image, seismic signals, and biomedical signal. But the high frequency parts can be decomposed by WPD, and the decomposition is neither redundant nor omissive. So the signal containing a large number of middle and high frequency can be better made time-frequency localization analysis by WPD. Because the milling force signal is non-stationary and high-frequency signal, the method of WPD can be used to obtain the chatter frequency.

Wavelet packet decomposition algorithm is given as

$$\begin{cases} d_{j,k}^{2n} = \sum_{t \in Z} \bar{h}_{t-2k} d_{j-1,t}^n \\ d_{j,k}^{2n+1} = \sum_{t \in Z} \bar{g}_{t-2k} d_{j-1,t}^n \end{cases} \quad (4)$$

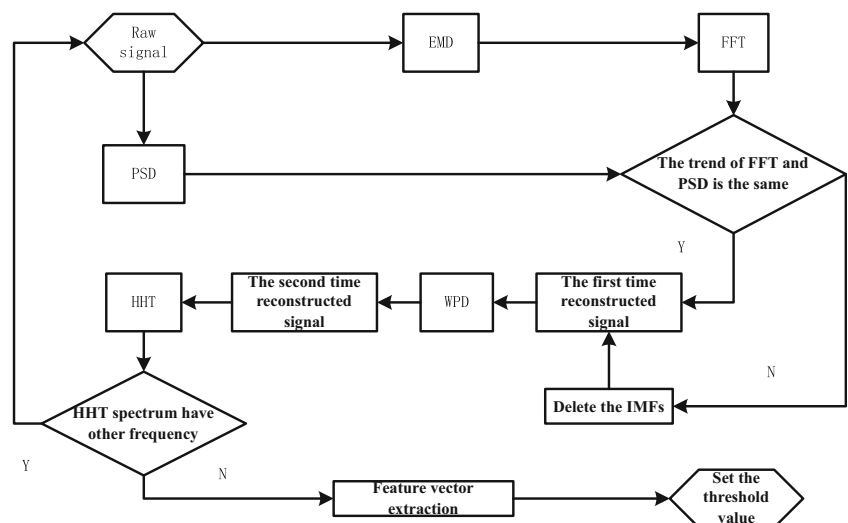
where $d_{j,k}^{2n}$ and $d_{j,k}^{2n+1}$ are wavelet packet coefficients, \bar{h}_{t-2k} and \bar{g}_{t-2k} are derivatives of filter coefficients. Wavelet packet reconstruction algorithm is given as

$$d_{j+1,k}^n = \sum_k [h_{t-2k} d_{j,k}^{2n} + g_{t-2k} d_{j,k}^{2n+1}] \quad (5)$$

3 Proposed chatter detection methodology

The IMFs which change only with the signal itself can be obtained by EMD, but IMFs are prone to modal aliasing. To solve

Fig. 1 The flow chart of the method of combining EMD and WPD to extract chatter features



this problem, the methods of EEMD and support vector machine (SVM) regression prediction and the largest Lyapunov exponent and so on are used. If the IMFs with modal aliasing are processed by WPD, the mixed modal will be identified. Based on this idea, the method of chatter identification is presented in this paper, which is shown in Fig. 1. First of all, the signal containing the chatter information is structured or measured by experiments. Then, the features of the IMFs are presented by EMD, FFT of IMFs and the power spectral density (PSD) are compared, FFT of IMFs changing consistent with PSD is selected to reconstruct the signal for the first time. If not, the IMFs will be deleted when the first time to reconstruct the signal. To eliminate the modal aliasing effect caused by EMD and subdivide the high frequency, the reconstructed signal is decomposed by WPD. The time-frequency diagram of the wavelet packet nodes is drawn by WPD. If the chatter happens, the maximum energy will be consumed. So the node with the maximum energy is chosen to reconstruct signal for the second time. Then, the second time reconstructed signal is processed by the HHT. If the HHT spectrum has some frequency bands, the above steps need to be repeated until a single frequency band. The resulting frequency band is chatter frequency band. In order to direct efficiently express chatter features, mathematical statistics and analysis of feature vector will be made. Based on this, the threshold is set to judge whether chatter happens.

4 The chatter features extraction of simulation signal

In order to show the effectiveness of the above method, the signal with chatter frequency is simulated by:

$$y = 4\sin(74\pi t) + 5\sin(30\pi t) + 0.5(1 + 0.6\sin(30\pi t))\cos(300\pi t + 1.5\sin(15\pi t)) \quad (6)$$

The simulation signal is shown in Fig. 2. The chatter signal contains three parts: the sinusoidal curves are shown by the first two parts, which represent the spindle frequency and tooth passing frequency, the chatter signal is performed by the third part.

4.1 PSD analysis

The signal is given by $x(n), E[x(n)] = \frac{1}{2\pi} \int_{-\pi}^{\pi} P_{xx}(w)dw$, where $E[x(n)]$ represents the average signal power, and where $P_{xx}(w)$ is proportional to the average signal power in $-\pi \leq w \leq \pi$. So the physical meaning of $P_{xx}(w)$ is the average power density of the signal, which is called the power spectrum density. The purpose of spectral analysis is to study the energy distribution at different frequencies. The auto-correlation function and the periodic chart are used to make spectral analysis. Algorithm of autocorrelation function method is given as:

$$P_N(w) = \sum_{m=-(N-1)}^{N-1} r_N(m) e^{-jwm} \quad (7)$$

Among them, $P_N(w)$ is the power spectral density of the fourier transform, $r_N(m)$ is a self -correlation function. For random sequence $x(n)$ of the long N , the specific is divided into two steps, (1) the estimated value of the autocorrelation function can be given as,

$$r_N(m) = \frac{1}{N} \sum_{n=0}^{N-1-m} x(n)x(n+m), 0 \leq m \leq N-1 \quad (8)$$

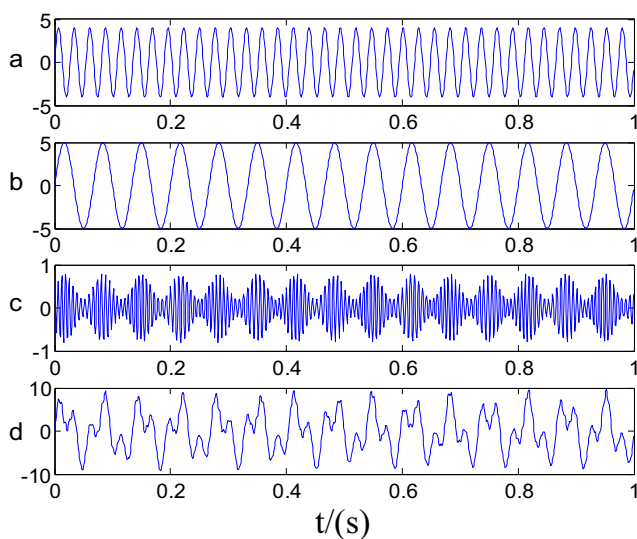


Fig. 2 The composition of simulation signal: **a** high frequency sinusoidal signal, **b** low frequency sinusoidal signal, **c** modulation signal, and **d** simulation signal

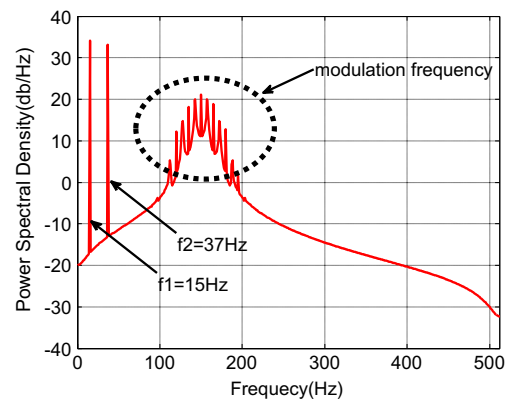


Fig. 3 The power spectrum of simulation signal

For the simulation signals, the power spectrum is obtained by the auto-correlation method, and the larger power spectrum appears in the $f_1 = 37$ Hz, $f_2 = 15$ Hz and the modulation frequency in Fig. 3.

4.2 Acquisition of IMFs and reconstruction of signal

The ultimate goal of EMD is to obtain the IMFs. The IMFs are shown in Fig. 4. The spindle frequency, the tooth passing frequency and modulation frequency of the signal can be decomposed, respectively, frequency bands are IMF1, IMF2, and IMF3 from high to low. To choose IMFs which can represent the main component of the original signal to reconstruct, the amplitude-frequency analysis of the IMFs are shown in Fig. 5. By comparison, the chatter frequency can be fully expressed by IMF1, and the spindle frequency and tooth passing frequency are expressed respectively by the IMF2 and IMF3. So IMF1 is selected to reconstruct the signal.

In addition, there exists another way to select the IMFs. If the chatter occurs during the cutting process, the energy will shift to the chatter frequency band. It is indicated that the

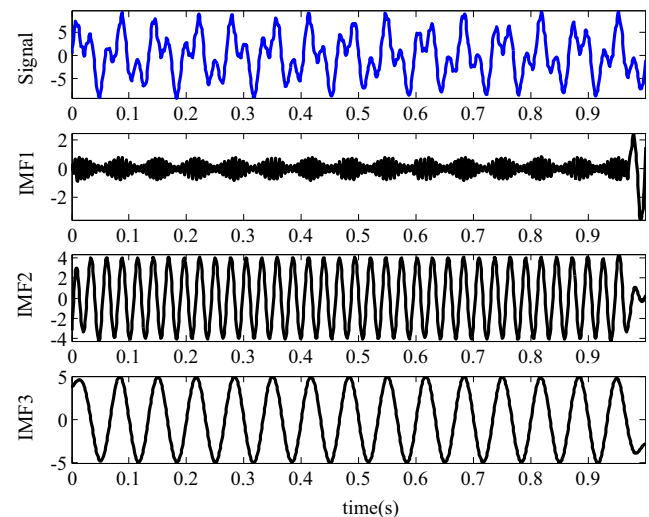


Fig. 4 The original signal and IMFs

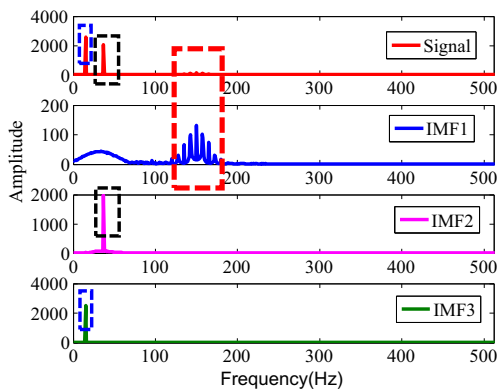


Fig. 5 Amplitude-frequency characteristic of IMFs

change trend of amplitude-frequency characteristic and PSD are the same. By comparing the amplitude-frequency characteristic and PSD of each IMF, the change trend of the IMFs, which are the same as PSD's, can be chosen to reconstruct the signal.

4.3 WPD analysis and two times reconstruction of signal

In order to eliminate the modal aliasing of EMD and get further information of chatter frequency, WPD is used to extract chatter frequency. The db3 is used as wavelet basis, three levels are selected to analyze. So frequency bands of the 7–14 node are 0–64 Hz, 64–128 Hz, 128–192 Hz, 192–256 Hz, 256–320 Hz, 320–384 Hz, 384–448 Hz, 448–512 Hz. The frequency band of IMFs will be further subdivided by WPD, and mixed modals are separated. The time-frequency diagram is drawn in Fig. 6 based on energy of the frequency band:

It can be seen from Fig. 7, energy is mainly concentrated in the 10th node, the frequency with 192–256 Hz, and the rest energy is concentrated in the 8th node (64–128 Hz) and the 7th node (0–64 Hz), so the 10th node is selected for signal reconstruction, the reconstructed signal is shown in Fig. 7.

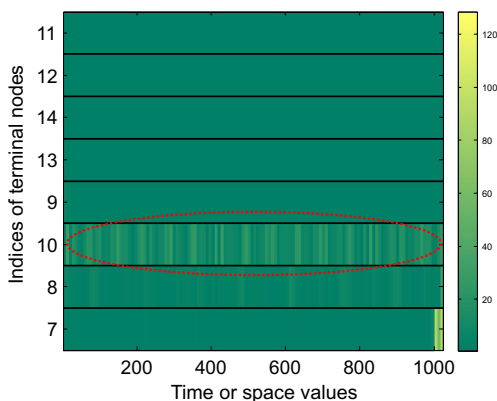


Fig. 6 Time frequency diagram of the wavelet packets nodes

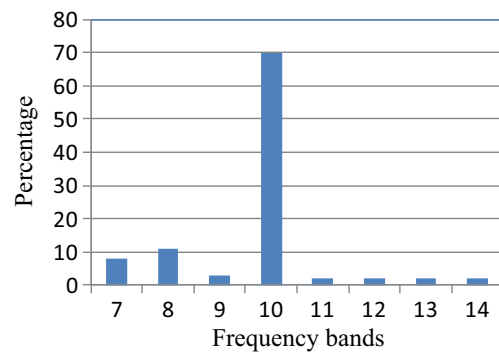


Fig. 7 The percentage of frequency bands

The period of the reconstructed signal in Fig. 8 can be seen, that is, $T = 15$, so the chatter information is represented by the reconstructed signal. In addition, the amplitude of reconstructed signal is in $[-1, 1]$, the amplitude of raw signal is in $[-10, 10]$, some useless information including spindle frequency and tooth passing frequency are deleted by the first time reconstructed signal.

4.4 HHT spectrum analysis and chatter feature vectors

EMD is based on the local characteristic of time scale of the signal, and EMD is an adaptive decomposition. The signal is decomposed by EMD into several IMFs, which makes that the instantaneous frequency of the concept has the practical significance. So the instantaneous frequencies and amplitudes of each IMF can be calculated. Hilbert transform is given as,

$$\hat{h}_i(t) = \frac{1}{\pi} \int_{-\infty}^{\infty} \frac{h_i(t)}{t-\tau} d\tau \tag{9}$$

Structural analytical signal is given as:

$$z_i(t) = h_i(t) + j \hat{h}_i(t) = a_i(t)e^{j\theta_i(t)} \tag{10}$$

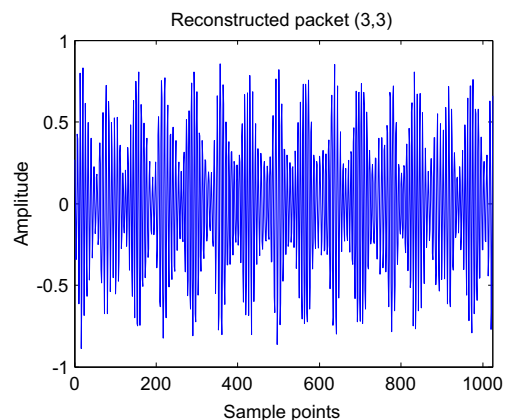


Fig. 8 The first time to reconstruct the signal with the 10th node

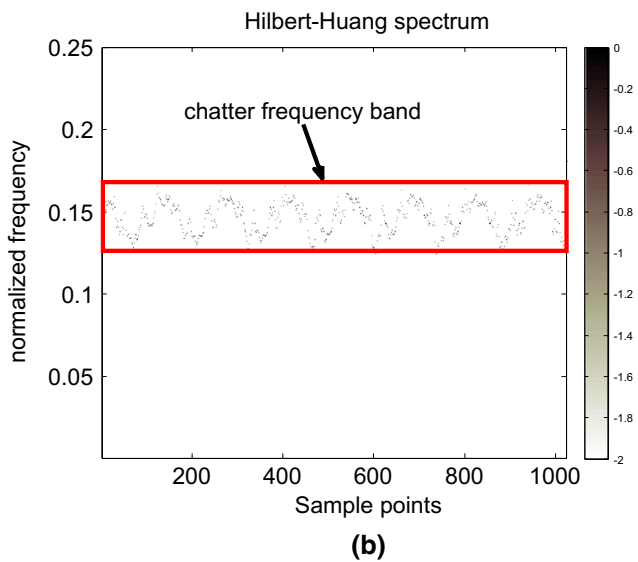
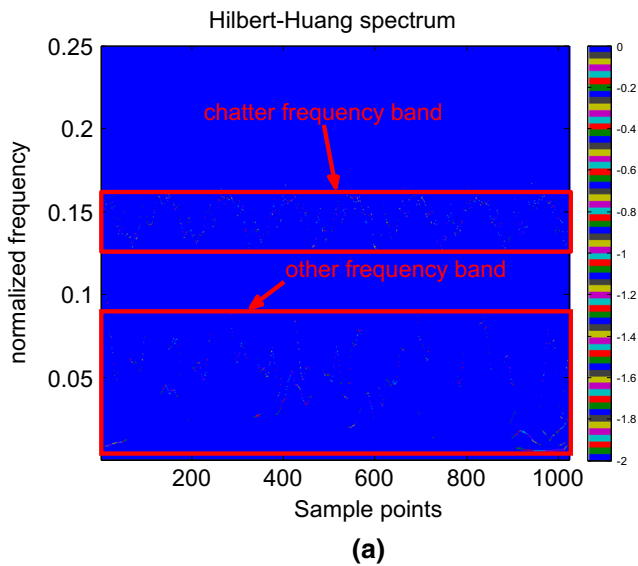


Fig. 9 HHT spectrum of **a** the second time reconstructed signal and **b** the fourth time reconstructed signal

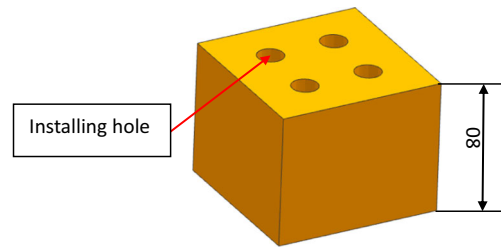


Fig. 11 The geometry of the workpiece

Further the instantaneous frequency is obtained by:

$$f_i(t) = \frac{1}{2\pi} w_i(t) = \frac{1}{2\pi} \times \frac{d\phi_i(t)}{dt} \tag{11}$$

So the instantaneous frequency can be obtained by HHT spectrum. HHT spectrum of the second time and the fourth time reconstructed signals is shown in Fig. 9.

In Fig. 9a, the chatter frequency can be clearly seen from the second time reconstructed signal, but the other frequency also can be seen too. To obtain a single frequency band, the above steps are repeated. The details have been expressed in part 3. A single frequency band can be seen from Fig. 9b. So the method can be effectively used to extract the chatter features. The mean value and standard deviation of HHT spectrum are extracted as feature vectors, respectively, the mean value of the frequency is $0.1464 \times 512 = 75$ Hz and standard deviation is $0.0094 \times 512 = 4.8128$ Hz.

5 Results and analysis of milling experiment

5.1 Experimental setup

The proposed chatter identification methodology has been validated on a CNC milling machine named DMU50 (Fig. 10), the diameter of cutter used in test is $D = 10$ mm, whose number of teeth are $N = 4$. The aluminum alloy ($100 \text{ mm} \times 100 \text{ mm} \times 80 \text{ mm}$) is slot milled. The geometry of workpiece is shown in Fig. 11. Kistler 9257B is used to

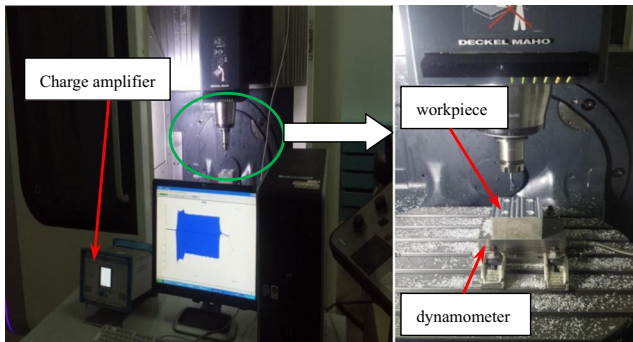


Fig. 10 The milling experimental platform

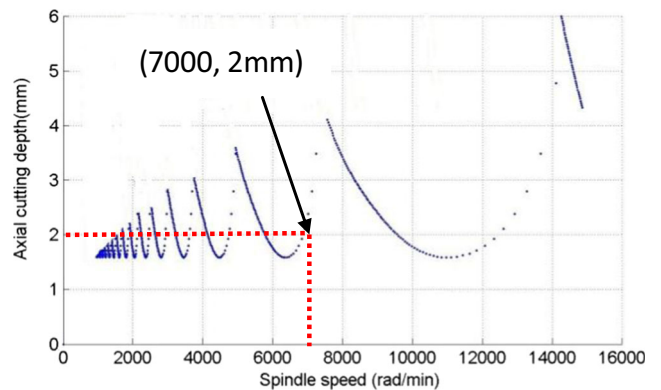


Fig. 12 The stability lobes diagram

Table 1 The cutting parameters

Experimental group number	Spindle speed n (r/min)	axial cutting depth a_p (mm)	feed rate F (mm/min)
1	7000	1	700
2	7000	2	700
3	7000	3	700

collect the force signal, which can measure forces in x , y , and z axis. The dynamometer is fixed by pressure plate and both are on the workbench, and the workpiece and the dynamometer are fixedly connected with the bolt. In order to make the dynamometer accurate, the dynamometer is preheated more than half an hour. The whole cutting process is carried out under dry milling conditions.

In the experiment, the milling force is affected by the milling parameters such as axial cutting depth a_p , feed rate F , speed n , and so on, but the change of the milling force is the greatest influenced by the axial cutting depth. To well select the cutting parameters, the stability lobes diagram (SLD) is drawn based on the modal tests. The SLD is shown in Fig. 12. The cutting parameters are shown in Table 1.

Three cutting conditions (stable cutting, slight chatter, severe chatter) are represented by three groups of the milling experiment in which the axial cutting depth is changed.

5.2 Results and analysis

The measured signals are shown in Fig. 13. It can be seen that with the increase of cutting depth, the amplitude of cutting force increases. The three cutting conditions (stable cutting,

Fig. 13 The milling force F_x of three groups

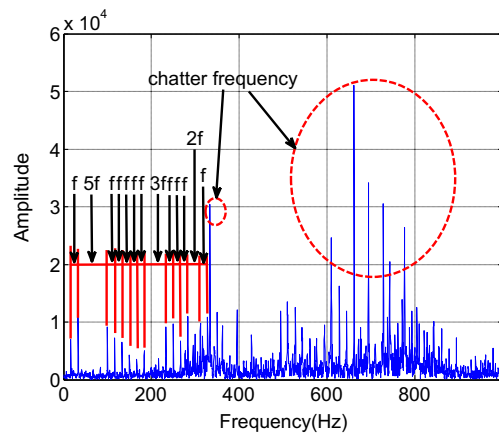
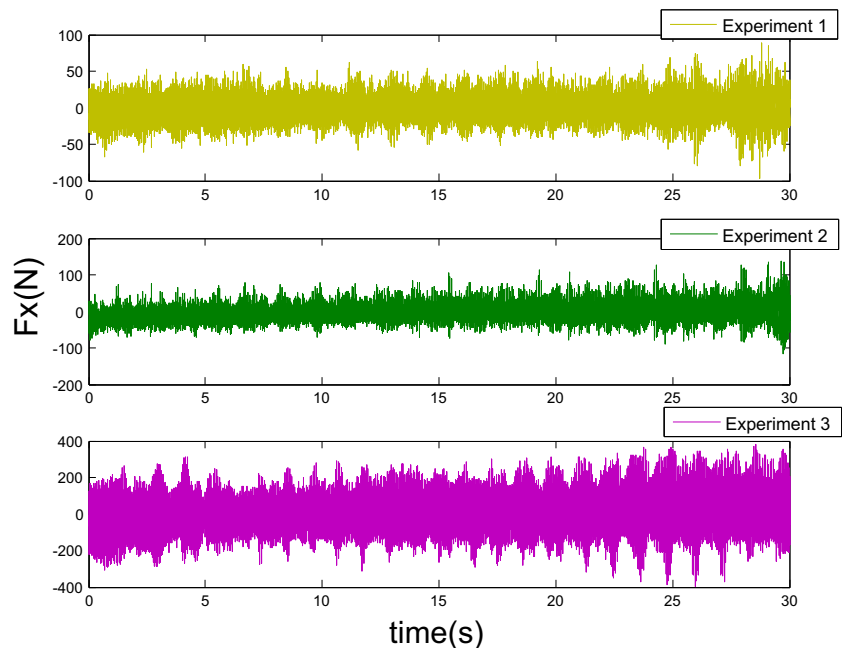
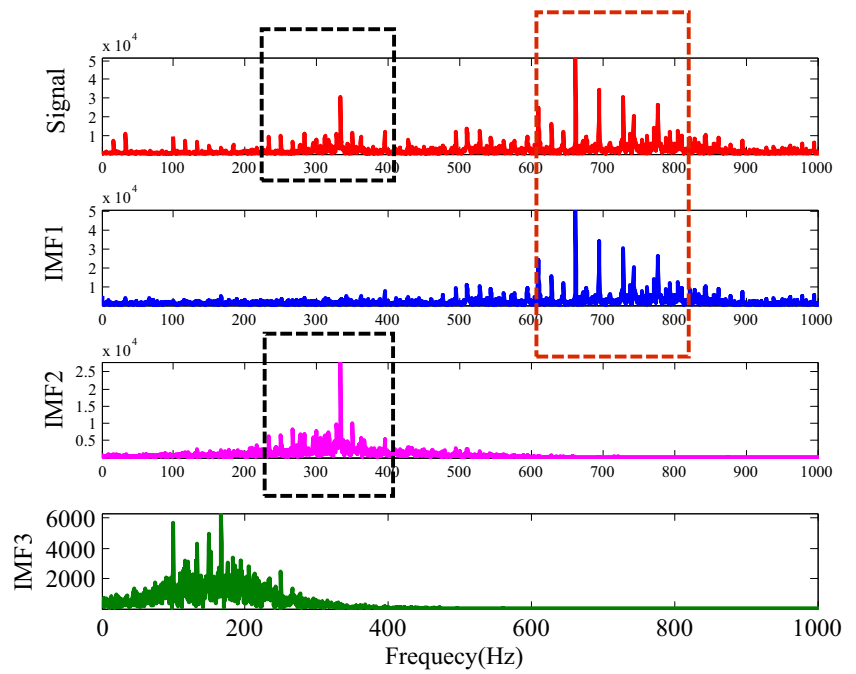


Fig. 14 The FFT of the third group

slight chatter, and severe chatter) are verified by the FFT. During the stable cutting, the vibration is mainly focused on the spindle frequency (also called dominant frequency), the tooth passing frequency, and the resonant frequency. When the chatter occurs, the vibration will be focused on the chatter frequency. The FFT of the third group is shown in Fig. 14, where the chatter frequency is marked and the spindle frequency is denoted by f . The spindle frequency of machine is stimulated by tool, which belongs to a forced vibration. If the tool has two teeth, the tooth passing frequency will be two times of the spindle frequency. The frequency of forced vibration is the integer multiples of spindle frequency. The chatter frequency is not the integer multiples of spindle frequency. In FFT, the frequency, which has the larger amplitude and not the integer multiples of dominant frequency, is chatter frequency. Next, according to the method of combining EMD and WPD

Fig. 15 The amplitude-frequency characteristic of IMFs in third groups



proposed in this paper, the EMD is done. The FFT of first three IMFs is shown in Fig. 15. It can be concluded rich chatter information is contained in IMF1, spindle frequency, and tooth passing frequency and the resonance frequency is contained in IMF2 and IMF3.

As discussed before, IMF1 is used for the first time to reconstruct signal. Then, for the elimination of modal aliasing phenomenon and further subdivision of the frequency, WPD of the first time reconstructed signal is made. Based on the energy distribution of the wavelet packet nodes, the node with the maximum energy distribution is selected for the second time to reconstruct the signal. The second time reconstruction of the third group is shown in Fig. 16. It can be seen that the amplitude of the second time reconstructed signal is very clear. Next, the signal is analyzed by HHT transform, which aim is to determine the frequency distribution in the time

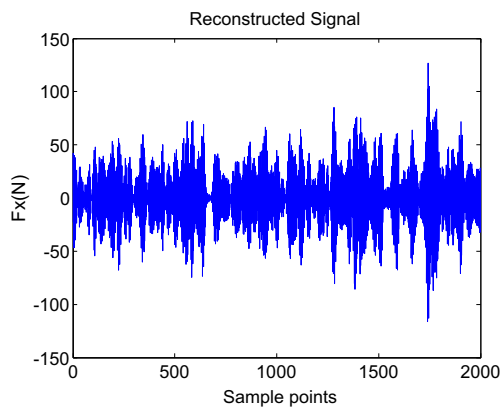


Fig. 16 The second time reconstructed signal

domain. The HHT spectrum of groups 1, 2, 3 are respectively shown in Table 2.

It can be concluded from Table 2, with increase of cutting depth, the frequency band is becoming more and more narrow. In the stable cutting condition, the frequency components distribute dispersedly in the range of normalized frequency 0.18–0.22. In the slight chatter case, the frequency components gather a little. In the severe chatter case, the features are quite clear. The frequency components almost gather in a line. It can be seen that HHT after EMD and WPD can be used efficiently for chatter detection. Although it is obvious to identify chatter from Hilbert-Huang spectrum, the mathematical features is simple to judge. The mean value and standard deviation of the Hilbert-Huang spectrum are calculated to find proper indices for chatter identification, which is listed in Table 3. When chatter happens, the vibration is strengthened and the mean value will be increased. When chatter happens, the vibration energy is centralized around the chatter frequencies and hence the uneven degree is increased, which lead to increase of the standard deviation. In the stable cutting process, the mean value and standard deviation are 699.3 and 0.0141. In the slight chatter case, the mean value and standard deviation are increased to 708.75 and 0.0184, and in the severe chatter case, these values are increased to 715.75 and 0.0241. Therefore, the mean value and standard deviation of

Table 2 The HHT spectrum of three cutting parameters

	Stable cutting (Group 1)	Slight chatter (Group 2)	Severe chatter (Group 3)
Normalized frequency	0.18–0.22	0.19–0.21	0.198–0.203

Table 3 The mean and standard deviation of three cutting parameters

	Stable cutting (Group 1)	Slight chatter (Group 2)	Severe chatter (Group 3)
Mean value (Hz)	699.3	708.75	715.75
Standard deviation	0.0141	0.0184	0.0241

the Hilbert-Huang spectrum can be used as indices to simply identify the chatter.

More cutting tests are carried out under the same cutting condition (i.e., spindle speed 7000 r/min, feed rate 700 mm/min, slotting), the threshold of mean value is set to 710 Hz, the threshold of standard deviation is set to 0.02. If the mean value and standard deviation is higher than the threshold value, it will show that chatter has already happened in the milling process.

6 Conclusions

To eliminate the influence of modal aliasing and subdivide the frequency after EMD, the chatter identification method of combining EMD and WPD is proposed in this paper. The IMFs changing consistent with PSD or amplitude-frequency are selected for the first time reconstruction. The second time reconstruction is based on wavelet packet node with the maximum energy. In this way, the energy and frequency distribution features of the whole milling process can fully be expressed by the reconstructed signal. Contrast to Cao's method, the method can get a single frequency band which don't contain other frequency bands.

- 1) The other frequency band can also be seen from HHT spectrum of the second time reconstructed signal. To eliminate the influence of the other frequency band and subdivide the frequency, the method of combining EMD and WPD is repeated until a single frequency band. So the method of combining EMD and WPD is needed to be repeated at least once.
- 2) During the milling process, if the chatter occurs, the energy will be redistributed, and the energy will be concentrated to the chatter frequency. From the analysis of the chatter feature vector, it can be seen that the mean value and standard deviation of the HHT spectrum can be used as indicators to identify chatter.
- 3) The trend of amplitude-frequency curve and PSD of milling force signal is the same. So the IMFs can be chosen by comparing the amplitude-frequency feature and signal itself.

Acknowledgments This work was supported by the National Natural Science Foundation of China (NSFC) (51105072 and 51475087), supported by the Fundamental Research Funds for the Central Universities (N150304005).

References

1. Compeán FI, Olvera D, Campa FJ, Lacalle LNL, Elías-Zúñiga A, Rodríguez CA (2012) Characterization and stability analysis of a multivariable milling tool by the enhanced multistage homotopy perturbation method. *International Journal of Machine Tools & Manufacture* 57:27–33
2. Urbikain G, Fernández A, Lacalle LD (2013) Stability lobes for general turning operations with slender tools in the tangential direction. *International Journal of Machine Tools & Manufacture* 67:35–44
3. Urbikain G, Campa FJ, Zulaika JJ, Lacalle LNL, Alonso MA, Collado V (2015) Preventing chatter vibrations in heavy-duty turning operations in large horizontal lathes. *Journal of Sound & Vibration* 340:317–330
4. Wan M, Ma YC, Zhang WH, Yang Y (2015) Study on the construction mechanism of stability lobes in milling process with multiple modes. *Int J Adv Manuf Technol* 79:1–15
5. Yue C, Liu X, Liang SY (2016) A model for predicting chatter stability considering contact characteristic between milling cutter and workpiece. *Int J Adv Manuf Technol* 3:1–10
6. Yang Y, Zhang WH, Ma YC, Wan M (2016) Chatter prediction for the peripheral milling of thin-walled workpieces with curved surfaces. *International Journal of Machine Tools & Manufacture* 109:36–48
7. Wan M, Ma YC, Feng J, Zhang WH (2016) Study of static and dynamic ploughing mechanisms by establishing generalized model with static milling forces. *Int J Mech Sci* 114:120–131
8. Wan M, Wang YT, Zhang WH, Yang Y, Dang JW (2011) Prediction of chatter stability for multiple-delay milling system under different cutting force models. *International Journal of Machine Tools & Manufacture* 51:281–295
9. Wan M, Altintas Y (2014) Mechanics and dynamics of thread milling process. *International Journal of Machine Tools & Manufacture* 87:16–26
10. Bustillo A, Lacalle LNL, Fernández-Valdivielso A, Santos P (2016) Data-mining modeling for the prediction of wear on forming-taps in the threading of steel components. *Journal of Computational Design & Engineering* 3:337–348
11. Álvar AG, Fernández VA, Bustillo A, Lacalle LNL (2016) Using artificial neural networks for the prediction of dimensional error on inclined surfaces manufactured by ball-end milling. *Int J Adv Manuf Technol* 83:847–859
12. Miran B, Miha K (2003) Integrated genetic programming and genetic algorithm approach to predict surface roughness. *Mater Manuf Processes*, 18:475–491
13. Yildiz AR (2013) Cuckoo search algorithm for the selection of optimal machining parameters in milling operations. *Int J Adv Manuf Technol* 64:55–61
14. Escamilla-Salazar IG, Torres-Treviño LM, González-Ortiz B, Zambrano PC (2012) Machining optimization using swarm intelligence in titanium (6al 4v) alloy. *Int J Adv Manuf Technol* 67:535–544
15. Yamada Y, Kakinuma Y (2016) Sensorless cutting force estimation for full-closed controlled ball-screw-driven stage. *Int J Adv Manuf Technol*. doi:10.1007/s00170-016-8710-5
16. Khasawneh FA, Munch E (2016) Chatter detection in turning using persistent homology. *Mechanical Systems & Signal Processing* 70:527–541
17. Matthias W, Özşahin O, Altintas Y, Denkena B (2016) Receptance coupling based algorithm for the identification of contact parameters at holder-tool interface. *Cirp Journal of Manufacturing Science & Technology* 13:37–45
18. Siddhpura M, Paurobally R (2012) A review of chatter vibration research in turning. *Int J Mach Tools Manuf* 6:27–47

19. Urbański T, Kossakowska J, Jemielniak K (2010) Application of wavelet transform of acoustic emission and cutting force signals for tool condition monitoring in rough turning of Inconel 625. *Proc Inst Mech Eng B J Eng Manuf* 1:1–7
20. Litak G, Kecik K, Rusinek R (2013) Cutting force response in milling of Inconel: Analysis by wavelet and Hilbert-Huang transforms. *Latin American Journal of Solids and Structures* 10:133–140
21. Karam S, Teti R (2013) Wavelet transform features extraction for chip form recognition during carbon steel turning. *Procedia CIRP* 12:97–102
22. Meignen S, Oberlin T, Depalle P, McLaughlin S (2016) Adaptive multimode signal reconstruction from time-frequency representations. *Philosophical Transactions of the Royal Society A Mathematical Physical & Engineering Sciences* 374:2065
23. Yao Z, Mei D, Chen Z (2010) On-line chatter detection and identification based on wavelet and support vector machine. *J Mater Process Technol* 210:713–719
24. Peng C, Wang L, Liao TW (2015) A new method for the prediction of chatter stability lobes based on dynamic cutting force simulation model and support vector machine. *Journal of Sound & Vibration* 354:118–131
25. Fang N, Pai PS, Mosquea S (2010) Effect of tool edge wear on the cutting forces and vibrations in high-speed finish machining of Inconel 718: an experimental study and wavelet transform analysis. *Int J Adv Manuf Technol* 52:65–77
26. Huang P, Li J, Sun J, Zhou J (2013) Vibration analysis in milling titanium alloy based on signal processing of cutting force. *Int J Adv Manuf Technol* 64:613–621
27. Wei CC, Liu MK, Huang GH (2016) Chatter identification of face milling operation via time-frequency and fourier analysis. *International Journal of Automation and Smart Technology* 6:25–36
28. Zhang Z, Li H, Meng G, Tu X, Cheng C (2016) Chatter detection in milling process based on the energy entropy of VMD and WPD. *International Journal of Machine Tools & Manufacture* 108:106–112
29. Rafał R, Paweł L, Krzysztof K, Bogdan K, Jerzy W (2015) Chatter identification methods on the basis of time series measured during titanium superalloy milling. *Int J Mech Sci* 99:196–207
30. Cao HR, Lei Y, He Z (2013) Chatter identification in end milling process using wavelet packets and Hilbert-Huang transform. *Int J Mach Tools Manuf* 69:11–19
31. Cao HR, Zhou K, Chen X (2015) Chatter identification in end milling process based on EEMD and nonlinear dimensionless indicators. *Int J Mach Tools Manuf* 92:52–59
32. Fu Y, Zhang Y, Zhou H, Li D, Liu H, Qiao H (2016) Timely online chatter detection in end milling process. *Mech Syst Signal Process* 75:668–688
33. Yang YF, Wu YF (2013) Applications of empirical mode decomposition in vibration analysis. National Defence Industry Press, Beijing
34. Cao HR, Yue YT, Chen XF, Zhang XW (2016) Chatter detection in milling process based on synchrosqueezing transform of sound signals. *Int J Adv Manuf Technol* 1:1–9